Supplementary Results

Supplemental Figure I: miRNA qRT-PCR expression in the humanized balloon injury and stent-model.

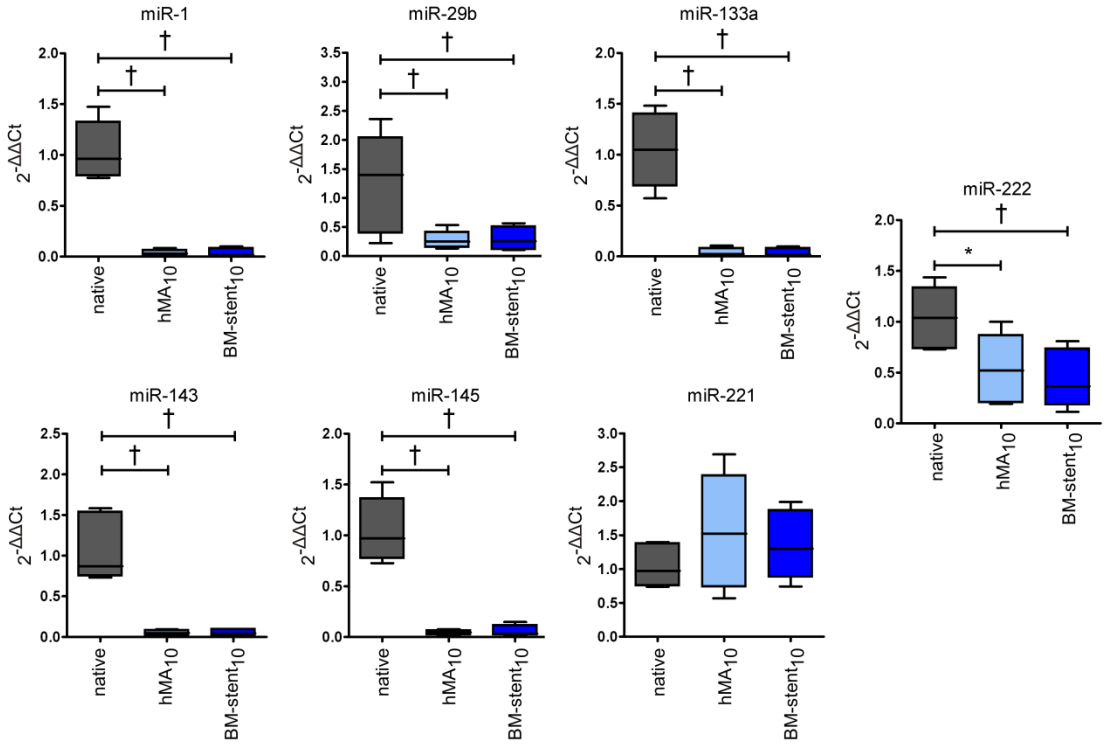

Human IMA were denuded with a 2 Fr. catheter (hMA) or had a stent deployed (BM-stent), followed by implantation into the abdominal aorta of RNU rats. miRNA expression was measured using qRT-PCR 10 days after implantation. Six of the evaluated miRNAs were differentially expressed compared to native IMA vessels. Significantly down-regulated miRNAs included: miR -1, miR-29b, miR-133a, miR-143, miR-145 and miR-222. Notably, stented hMA-vessels had similar expression profiles to balloon-denuded vessels. Thus, vessel injury in the humanized model resulted in a similar dysregulation of miRNA expression, regardless of additional stenting (mean± s.d., n=6 animals per group, ANOVA with Bonferroni's post-hoc test). * $p<0.05$, † $p<0.01$.

Supplemental Figure II: Off-target effects of systemic (A) and local (B) anti-21 treatment.

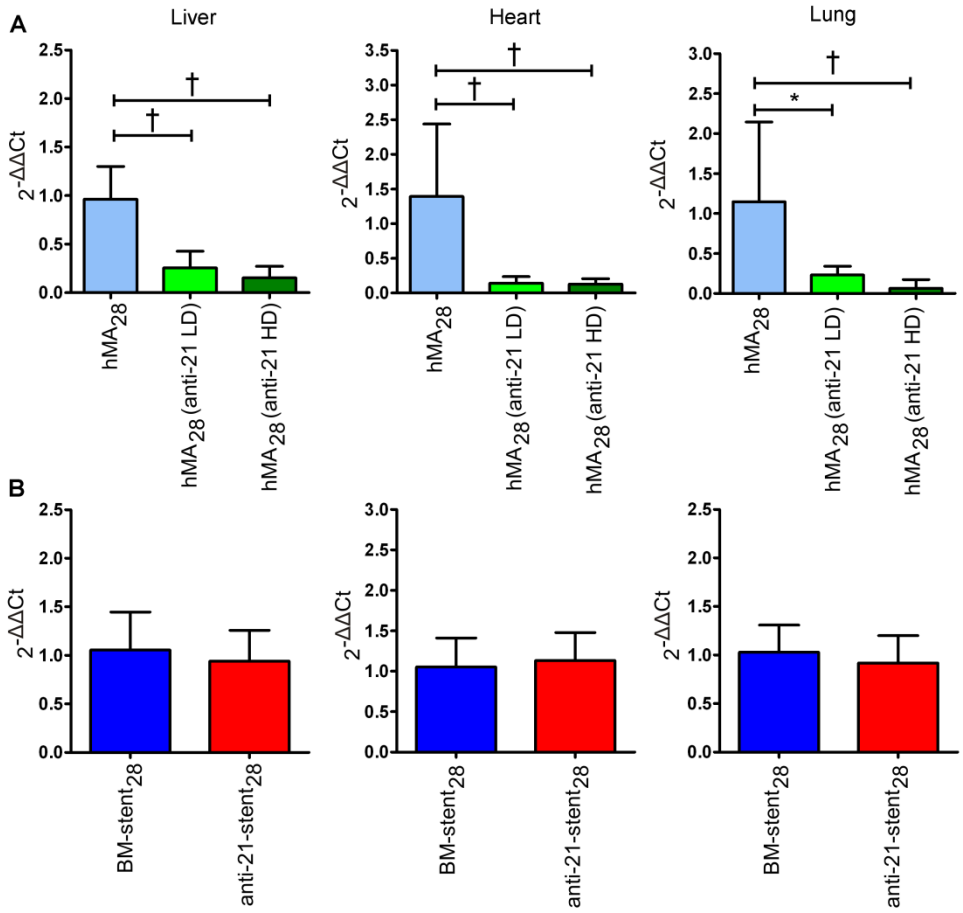

To evaluate potential off-target effects of anti-21 treatment, miR-21 expression in organs from systemically treated (A) and locally treated animals (B) were determined by qRT-PCR. Systemically treated animals showed considerably reduced miR-21 expression in the liver (mean± s.d., n=7 per group, ANOVA with Bonferroni's post-hoc test), heart (mean± s.d., n=6 (hMA), n=7 (anti-21 LD), n=6 (anti-21 HD), ANOVA with Bonferroni's post-hoc test) and lung (mean± s.d., n=7 per group, ANOVA with Bonferroni's post-hoc test). In contrast, no relevant differences were detected in the liver, heart and lung (mean± s.d., n=8 (BM-stent), n=6 (anti-21-stent), unpaired t-test) between the BM-stent group and the local anti-21-stent group, indicating no relevant off-target effects by local anti-21 delivery. *$p<0.05$, † $p<0.01$.

Supplemental Figure III: Confirmation of successful stent coating and humanized balloon injury and stent model

A

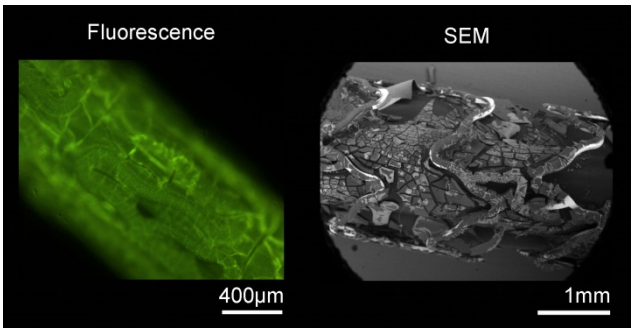

B

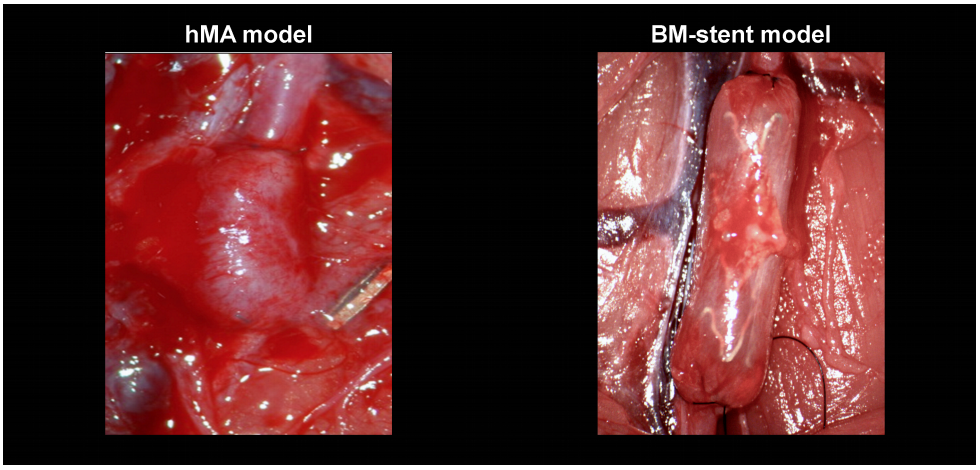

(A) FAM-tagged-LNA-anti-miR-21 (anti-21) was dissolved in 70% isopropyl alcohol and coated onto stents. Fluorescence (left) and scanning electron (right) microscope images, confirm successful anti-21-coating onto the stent surface. (B) Surgical technique of the hMA model (left): Human internal mammary arteries (IMA) were balloon injured with a 2 French catheter and implanted into the abdominal aortic position of RNU rats via end-to-end anastomosis. Surgical technique of BM-stent model (right): A stent was deployed into balloon-injured IMA, followed by implantation into the abdominal aorta of RNU rats.

Supplemental Figure IV: Immunohistochemical analysis of denuded, but untreated control arteries from the humanized mammary artery model (hMA), as well as anti-21 high dose treated rats (anti-21 HD), harvested 28 days after vessel wall injury.

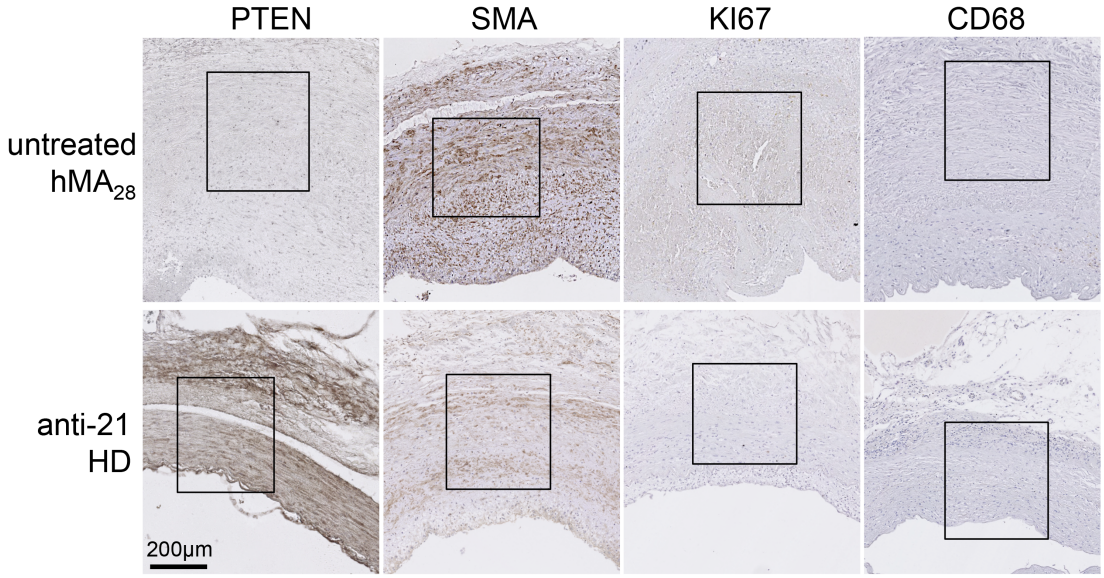

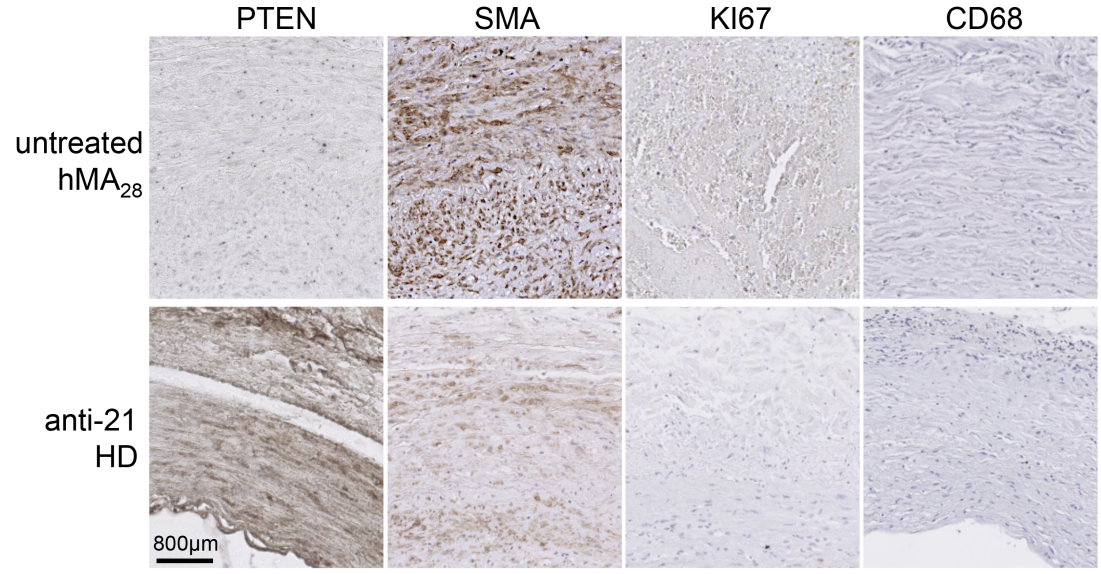

Immunohistochemistry analysis was performed with primary antibodies against PTEN (main target of miR-21 in myointimal hyperplasia formation), smooth muscle cell α-actin (SMA) and KI67 (both indicating the anti-21 treatment effect on SMC proliferation), and CD68 as a macrophage marker to display differences in the inflammatory response, which was not visibly altered with miRNA inhibition. Highlighted areas in upper figure are displayed in images below.

Movie S1: Optical coherence tomography (OCT) imaging video showing in-stent restenosis in BM-stent versus anti-21-stent. Motorized OCT pullbacks were performed at a rate of 1 mm/s and images were acquired at 15 frames/s. Images revealed considerably less myointima formation in the anti-21-stent group (right) compared to BM-stent (left).